3) 横関 博雄、接触皮膚炎診療ガイドラインダイジェスト、 最新の疾患別治療マニュアル、19-20、2012
4) 佐藤 貴浩, 横関 博雄, 片山 一朗, 室田 浩之, 新樹, 朴 紀央, 椛島 健治, 中溝 聡, 高森 建二, 塩原 哲夫, 三橋 善比古, 森田 栄伸、日本皮膚科学会ガイドライン 慢性痒疹診療ガイドライン： Source：日本皮膚科学会雑誌 122： 1-16、2012.
5) 横関 博雄、最新の膠原病診療-そのパラダイムシフト】ステロイド外用薬の使い方と留意点、日本医師会雑誌：140、2331-2335、2012.
6) 横関博雄：皮膚アレルギー疾患における核酸医薬療法、Jpn J Clin Immunol,35(2)107-111,2012
7) 加藤恒平、田中智子、佐藤貴浩、横関博雄:【アトピー性皮膚炎-2012】 アトピー性皮膚炎の患者に発症した減汗性コリン性蕁麻疹、皮膚病診療 34:33-36, 2012
8) 春山興右、高橋英至、上田暢彦、佐藤貴浩、横関博雄：エビによる食物依存性運動誘発アナフィラキシーの 1 例、臨床皮膚科 66:19-23, 2012
9) 藤本智子、宗次太吉、横関博雄、菅野範英、吉岡洋：原発性局所多汗症術後代償性発汗のアンケート集計結果、発汗学 19:36-39, 2012

Ⅳ．研究成果の刊行に関する一覧表

別紙４

研究成果の刊行に関する一覧表レイアウト

雑誌

発表者氏名	論文タイトル名	発表誌名	巻号	ページ	出版年
小豆澤　宏明	【重症薬疹の診断と治療】 薬疹におけるリンパ球刺激試験でとらえる薬剤特異的T細胞	臨床免疫・アレルギー科	59巻4号	438-444	2013
小豆澤　宏明	薬疹を診る-注意点とその対応】最近の薬疹　注意すべき薬剤とその臨床症状	日本医師会雑誌	142巻3号	503-507	2013
Nakajima K, Terao M, Takaishi M, Kataoka S, Goto-Inoue N, Setou M, Horie K, Sakamoto F, Ito M, Azukizawa H, Kitaba S, Murota H, Itami S, Katayama I, Takeda J, Sano S.	Barrier abnormality due to ceramide deficiency leads to psoriasiform inflammation in a mouse model.	J Invest Dermatol.	133(11)	2555-65	2013
Hirobe S, Azukizawa H, Matsuo K, Zhai Y, Quan YS, Kamiyama F, Suzuki H, Katayama I, Okada N, Nakagawa S.	Development and clinical study of a self-dissolving microneedle patch for transcutaneous immunization device.	Pharm Res.	30(10)	2664-74	2013
Sakaguchi M, Bito T, Oda Y, Kikusawa A, Nishigori C, Munetsugu T, Yokozeki H, Itotani Y, Niguma T, Tsuruta D, Tateishi C, Ishii N, Koga H, Hashimoto T.	Three cases of linear IgA/IgG bullous dermatosis showing IgA and IgG reactivity with multiple antigens, particularly laminin-332.	JAMA Dermatol.	149(11)	1308-13.	2013
Inoue T, Yamaoka T, Murota H, Yokomi A, Tanemura A, Igawa K, Tani M, Katayama I.	Effective Oral Psoralen Plus Ultraviolet A Therapy for Digital Ulcers with Revascularization in Systemic Sclerosis.	Acta Derm Venereol.			2013
Takehara Y, Satoh T, Nishizawa A, Saeki K, Nakamura M, Masuzawa M, Kaneda Y, Katayama I, Yokozeki H.	Anti-tumor effects of inactivated Sendai virus particles with an IL-2 gene on angiosarcoma.	Clin Immunol.	149(1):	1-10.	2013
Saeki K, Satoh T, Yokozeki H.	α(1,3) Fucosyltransferases IV and VII are essential for the initial recruitment of basophils in chronic allergic inflammation.	J Invest Dermatol.	133(9)	2161-9.	2013
Hanafusa T, Matsui S, Murota H, Tani M, Igawa K, Katayama I.	Increased frequency of skin-infiltrating FoxP3+ regulatory T cells as a diagnostic indicator of severe atopic dermatitis from cutaneous T cell lymphoma.	Clin Exp Immunol.	172(3)	507-12.	2013
Kataoka N, Satoh T, Hirai A, Saeki K, Yokozeki H.	Indomethacin inhibits eosinophil migration to prostaglandin D2 : therapeutic potential of CRTH2 desensitization for eosinophilic pustular folliculitis.	Immunology.	140(1):	78-86.	2013

Kitagaki H, Hiyama H, Kitazawa T, Shiohara T.	Psychological stress with long-standing allergic dermatitis causes phychodermatological conditions in mice.	J Invest Dermatol.			2014
Takahashi R, Sato Y, Kurata M, Yamazaki Y, Kimishima M, Shiohara T	Pathological role of regulatory T cells in the initiation and maintenance of eczema herpeticum lesions	J Immunol	192	969-978,	2014
Hayakawa J, Mizukawa Y, Kurata M, Shiohara T	A syringotropic variant of cutaneous sarcoidosis: presentation of 3 cases exhibiting defective sweating responses.	J Am Acad Dermatol	68	1016- 1021	2013

Barrier Abnormality Due to Ceramide Deficiency Leads to Psoriasiform Inflammation in a Mouse Model

Kimiko Nakajima[1], Mika Terao[2], Mikiro Takaishi[1], Sayo Kataoka[3], Naoko Goto-Inoue[4,5], Mitsutoshi Setou[5], Kyoji Horie[6], Fumiko Sakamoto[7], Masaaki Ito[7], Hiroaki Azukizawa[2], Shun Kitaba[2], Hiroyuki Murota[2], Satoshi Itami[8], Ichiro Katayama[2], Junji Takeda[6] and Shigetoshi Sano[1]

It has been recognized that ceramides are decreased in the epidermis of patients with psoriasis and atopic dermatitis. Here, we generated Sptlc2 (serine palmitoyltransferase long-chain base subunit 2)-targeted mice (SPT-cKO mice), thereby knocking out serine palmitoyltransferase (SPT), the critical enzyme for ceramide biosynthesis, in keratinocytes. SPT-cKO mice showed decreased ceramide levels in the epidermis, which impaired water-holding capacity and barrier function. From 2 weeks of age, they developed skin lesions with histological aberrations including hyperkeratosis, acanthosis, loss of the granular layer, and inflammatory cell infiltrates. Epidermal Langerhans cells showed persistent activation and enhanced migration to lymph nodes. Skin lesions showed upregulation of psoriasis-associated genes, such as IL-17A, IL-17F, IL-22, S100A8, S100A9, and β-defensins. In the skin lesions and draining lymph nodes, there were increased numbers of γδ T cells that produced IL-17 (γδ-17 cells), most of which also produced IL-22, as do Th17 cells. Furthermore, IL-23-producing $CD11c^+$ cells were observed in the lesions. *In vivo* treatment of SPT-cKO mice with an anti-IL-12/23p40 antibody ameliorated the skin lesions and reduced the numbers of γδ-17 cells. Therefore, we conclude that a ceramide deficiency in the epidermis leads to psoriasis-like lesions in mice, probably mediated by IL-23-dependent IL-22-producing γδ-17 cells.

Journal of Investigative Dermatology (2013) **133,** 2555–2565; doi:10.1038/jid.2013.199; published online 11 July 2013

INTRODUCTION

Inflammatory skin diseases are often associated with disruption of the skin barrier function, although the cause and effect relationship is complex. The discovery of loss-of-function mutations in the *filaggrin* (*FLG*) gene in patients with atopic dermatitis (AD) revealed that disruption of the skin barrier is the primary cause of the disease (Palmer *et al.*, 2006; Irvine *et al.*, 2011). Similar to AD, the barrier function is altered in psoriasis although it remains unknown whether the abnormality of barrier function is a primary cause. Koebner phenomenon suggests that epidermal injury initiates the formation of psoriatic lesions. It is well known that occlusion (barrier restoration) reverses psoriatic lesions. Furthermore, multiple types of chronic barrier insults in experimental animals produce inflammation: for example, repeated tape stripping (TS); repeated applications of statins or lipid-secretion inhibitors; and essential fatty acid deficiency diet (Wood *et al.*, 1992; Feingold, 2007). Recent discoveries of the epidermal genes as psoriasis risk factors suggest the barrier abnormalities underlie the pathogenesis of psoriasis (Bergboer *et al.*, 2012). Among psoriasis model mice, some of them exhibit barrier dysfunction that links to altered immune response (Sano *et al.*, 2005; Hwang *et al.* 2012).

Stratum corneum (SC) lipids are derived from the contents of lamellar bodies (LBs) in granular cells and comprise a mixture of sphingolipids, cholesterol, and fatty acids, arranged as intercellular membrane bilayers that are required for the epidermal permeability barrier (Elias and Menon, 1991; Feingold, 2007). Ceramides play an essential role in the permeability barrier of the intercellular space and for the water retention of the SC (Elias and Menon, 1991). *De novo* synthesis of ceramides starts with a condensation of serine

[1]*Department of Dermatology, Kochi Medical School Kochi University, Nankoku, Japan;* [2]*Department of Dermatology, Osaka University Graduate School of Medicine, Suita, Japan;* [3]*Science Research Center, Kochi University, Nankoku, Japan;* [4]*Department of Health Promotion Sciences, Graduate School of Human Health Sciences, Tokyo Metropolitan University, Tokyo, Japan;* [5]*Department of Cell Biology and Anatomy, Hamamatsu University School of Medicine, Hamamatsu, Japan;* [6]*Department of Social and Environmental Medicine, Osaka University Graduate School of Medicine, Suita, Japan;* [7]*Division of Dermatology, Niigata University Graduate School of Medical and Dental Sciences, Niigata, Japan and* [8]*Department of Regenerative Dermatology, Osaka University Graduate School of Medicine, Suita, Japan*

Correspondence: Shigetoshi Sano, Department of Dermatology, Kochi Medical School, Kochi University, Kohasu, Okocho, Nankoku, Kochi 783-8505, Japan. E-mail:sano.derma@kochi-u.ac.jp

Abbreviations: cKO, conditional knockout; DETC, dendritic epidermal T cell; LB, lamellar body; LC, Langerhans cell; RT–PCR, reverse transcriptase PCR; SC, stratum corneum; SG, stratum granulosum; SPT, serine palmitoyltransferase; Sptlc2, serine palmitoyltransferase long-chain base subunit 2; TEWL, transepidermal water loss; TS, tape stripping; WT, wild type

Received 27 August 2012; revised 16 January 2013; accepted 23 January 2013; accepted article preview online 30 April 2013; published online 11 July 2013

and palmitoyl-CoA by serine palmitoyltranferase (SPT), the rate-limiting enzyme, which is ubiquitously found, including in the epidermis (Holleran *et al.*, 1990).

It has been reported that ceramides are significantly decreased in the epidermis of patients with psoriasis, as well as AD (Melnik *et al.*, 1988; Holleran *et al.*, 1991; Imokawa *et al.*, 1991; Motta *et al.*, 1993, 1994; Alessandrini *et al.*, 2004). SPT expression is significantly reduced in psoriatic lesions compared with uninvolved skin (Hong *et al.*, 2007). To investigate whether decrease of ceramide levels in the epidermis would lead to an inflammatory skin disease, we generated keratinocyte-specific *SPT* gene–targeted mice. The present study reveals a pathogenic link between the primary barrier disruption due to ceramide deficiency and immune responses that lead to psoriasis-like skin inflammation.

RESULTS

Decrease of ceramide levels in psoriatic epidermis and the generation of SPT-cKO mice

As previously recognized, psoriatic epidermis showed decreased ceramide levels compared with normal epidermis by immunostaining (Figure 1a). Correspondingly, the water-holding capacity and barrier function of the epidermis were impaired in psoriatic lesions compared with the uninvolved skin of patients with chronic, plaque-type psoriasis (psoriasis vulgaris) and control healthy skin (Figure 1b and c). As a previous study demonstrated that SPT is decreased in psoriatic lesions (Hong *et al.*, 2007), the decrease in ceramides may be, at least in part, due to the decrease in SPT level. As the Sptlc2 (serine palmitoyltransferase long-chain base subunit (2)) protein confers the catalytic activity of SPT (Dickson *et al.*, 2000), Cre/loxP-mediated targeting of the *Sptlc2* gene was undertaken under control of the K5 promoter to generate keratinocyte-specific SPT-targeted mice (Supplementary Figure S1a online; Tarutani *et al.*, 1997; Ohta *et al.*, 2009). Southern blot analysis and reverse transciptase (RT–PCR) verified the keratinocyte-specific targeting of the *Sptlc2* gene (Supplementary Figure S1b and c online). Newborn *K5-Cre: Sptlc2*$^{flox/flox}$ (SPT-cKO) mice presented with generalized xerosis (Figure 1d). However, their epidermis did not show any alteration in the histology or expression of K5, K1, K6, involucrin, filaggrin, or loricrin (Supplementary Figure S2 online). The water-holding capacity of SPT-cKO mice was reduced to 35% of the level found in wild-type (WT) mice ($P<0.001$, Figure 1e), whereas transepidermal water loss (TEWL) was unexpectedly normal at birth (Figures 2b and 3a). A novel method of imaging mass spectrometric analysis (Goto-Inoue *et al.*, 2012), which allowed us to identify ceramide species and their distribution, demonstrated a marked reduction of ceramide (Cer, d18:1/C24:1 at *m/z* 630.4) and ceramide-1-phosphate (Cer-1-P, d18:1/C18:0 at *m/z* 646.4) in the epidermis of footpad skin from SPT-cKO mice compared with those from WT mice (Figure 1f and g). Taken collectively, keratinocyte-specific SPT deficiency leads to a marked reduction of ceramide levels in the epidermis and constitutional impairment of hydration, although it does not affect skin barrier function or expression of epidermal differentiation molecules at birth.

SPT deficiency in keratinocytes impairs barrier recovery after TS

Electron microscopic examination revealed that LBs in newborn SPT-cKO mice showed a normal, disc-like appearance, but those in SPT-cKO mice at postnatal day 14 (PD14) had abnormal globular inclusions (Figure 2a). This result suggested that the defect in ceramide biosynthesis affected LB structure over time. Furthermore, the abnormal contents in LBs were similar to those with topical SPT inhibitor application (Holleran *et al.*, 1991). Previous studies demonstrated that SPT in the epidermis is required for barrier restoration (Holleran *et al.*, 1991, 1995). To verify this, the process of barrier recovery after TS of the skin was examined in SPT-cKO mice. As expected, SPT-cKO mice at PD3 demonstrated a significant elevation of TEWL at 2.5 h ($P=0.0029$) and at 6 h ($P=0.0002$) after TS, indicating a delay in barrier restoration in SPT-cKO mice compared with WT (Figure 2b). Electron microscopic examination at 6 h after TS revealed a delay in LB secretion into the extracellular space after TS, whereas in WT mice the intercellular lamellar units were regenerated (Figure 2c). These results suggest that LB secretion is dependent on SPT-dependent *de novo* synthesis of ceramides during the immediate barrier recovery. As ceramides could be provided from diet, for example, the barrier was restored by 24 h (Figure 2b).

Development of psoriasis-like skin lesions in SPT-cKO mice after 2 weeks of age

Although newborn SPT-cKO mice under steady state harbored an intact barrier function, it became disrupted and worsened from 2 weeks of age onward (Figure 3a). Correspondingly, electron microscopic examination demonstrated that numbers of LBs within keratinocytes in the granular layer significantly declined in SPT-cKO mice from 2 weeks onward (Figure 3b). After PD7, they showed growth retardation, sparse hair, and scales over their body (Figure 3c, left panel). SPT-cKO mice then developed alopecia in the periocular and upper back areas, and were covered with thick scales (Figure 3c, middle panel). From 3 weeks of age, the lesions deteriorated with alopecia, hyperkeratosis, and generalized erythema (Figure 3c, right panel). Most, if not all, SPT-cKO mice died by PD25. The skin histology of SPT-cKO mice from 2 weeks of age and older demonstrated a marked acanthosis, hyperkeratosis, loss of the granular layer, and cell infiltrates in the dermis (Figure 3d, bottom panel). Similar to psoriasis, there were a number of neutrophil infiltrates in the upper dermis and sub-to-intracorneal neutrophil accumulation resembling "the Munro's microabscess" (Supplementary Figure S3 online). Furthermore, similar to psoriatic lesions, K6 expression was observed in the whole layer of acanthotic epidermis in SPT-cKO mice (Figure 3e, bottom panel, Supplementary Figure S4b online), suggestive of an inflamed and hyperproliferative condition of the epidermis, whereas WT mice showed K6 only at the outer root sheath of hair follicles (Figure 3e, top panel). Interfollicular epidermal K6 was observed as early as PD6 in SPT-cKO, in which acanthosis did not yet develop, suggesting that ceramide deficiency might upregulate inflammatory signals (Supplementary Figure S4a online). On the other hand,

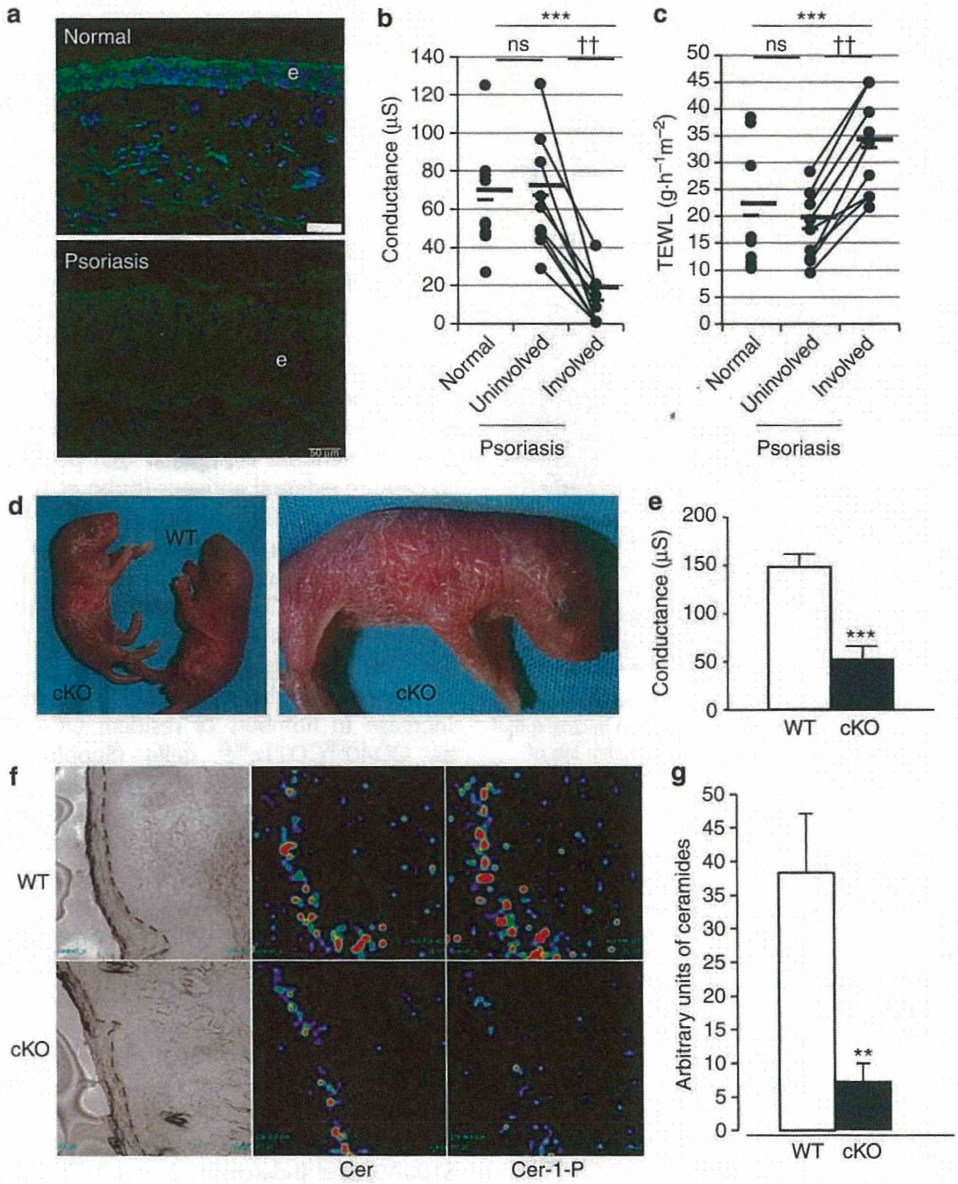

Figure 1. Decreased ceramides in the epidermis of psoriasis patients and the phenotype of newborn SPT-cKO mice. (**a**) Skin sections from a healthy subject (top) and a psoriasis patient (bottom) were stained with an anti-ceramide antibody. Ceramide levels were decreased in the thickened epidermis of the psoriasis patient compared with the normal healthy epidermis. Representative images are shown from three independent experiments. e, epidermis. Bar = 50 μm. (**b**, **c**) Involved skins ($n = 9$) from patients with chronic, plaque psoriasis (psoriasis vulgaris) show impaired water-holding capacity (**b**, evaluation by electrical conductance) and permeability barrier function (**c**, evaluation by transepidermal water loss) compared with uninvolved skins ($n = 9$) and normal skins from healthy donors ($n = 9$). Horizontal bars represent means. Statistical significance is indicated by $^{***}P < 0.001$. ns, not significant. Unpaired Student's *t*-test, and by $^{\ddagger\ddagger}P < 0.01$, Wilcoxon *t*-test. (**d**) Gross appearance of newborn wild-type (WT) and SPT-cKO (cKO) mice. (**e**) Decreased water retention in newborn SPT-cKO mice (black bar) compared with WT mice (white bar). Data show the mean conductance (μS) ± SE of three experiments with four to six mice each. $^{***}P < 0.001$. Unpaired Student's *t*-test. (**f**) Imaging mass spectrometry (IMS) analysis using footpad skin sections of SPT-cKO and WT mice at postnatal day (PD)3. Ion images of the epidermis of SPT-cKO mice revealed that ceramide (Cer, d18:1/C24:1 at *m/z* 630.4) and ceramide-1-phosphate (Cer-1-P, d18:1/C18:0 at *m/z* 646.4) were markedly decreased compared with WT mice. (**g**) Quantification of IMS signal intensity using ImageJ shows a significant decrease in the ceramide signal in SPT-cKO epidermis (black bar) compared with WT (white bar). Graph shows arbitrary units (mean ± SE). $n = 3$. $^{**}P < 0.01$. Unpaired Student's *t*-test.

distribution and expressions of cornified envelope proteins including involucrin, filaggrin, and loricrin remained intact in SPT-cKO mice over time with age (Supplementary Figure S4b online). Electron microscopic examination revealed a number of lipid inclusions in the SC, and vesicles in the stratum granulosum (SG) layer (Supplementary Figure S5a and b online). Notably, there were abnormal LBs and malformation of lamellar structures (Supplementary Figure S5c online). These changes resemble the ultrastructural alterations in active plaque psoriasis, in which corneocytes retain cytosolic LBs,

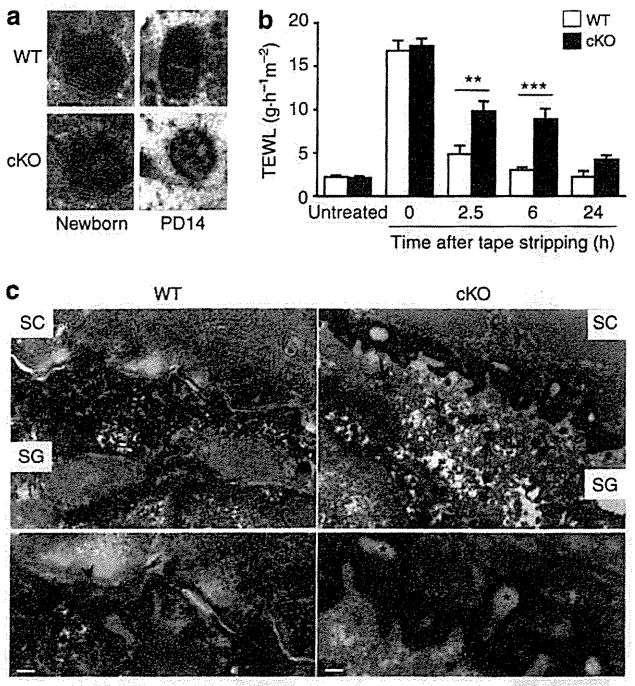

Figure 2. Alteration in the structure of lamellar bodies (LB) of SPT-cKO mice and delay in barrier recovery after tape stripping. (**a**) Electron micrograph of LBs. Note globular inclusions instead of lamellar formation within LBs of granular layer cells from SPT-cKO (cKO) mice at PD14, although those in newborn SPT-cKO mice show a normal appearance. Microphotographs are representative LBs from two mice with each genotype. Bar = 50 nm. Postfixed with RuO_4. (**b**) Delay in recovery from acute barrier disruption in 3-day-old SPT-cKO mice (black bars, $n = 23$) compared with age-matched control mice (white bars, $n = 20$). Graphs show transepidermal water loss (mean ± SE) at the indicated hours after tape stripping. $^{**}P < 0.01$; $^{***}P < 0.001$. Unpaired Student's *t*-test. (**c**) Electron micrographs of the epidermis at 6 h after tape stripping in SPT-cKO mice at PD3 (right panels) and in age-matched wild-type (WT) mice (left panels). Bottom panels are close-up views. At 6 h after tape stripping, when the barrier function is restored in WT mice, newly basic lamellar structures are formed at the stratum granulosum (SG)–stratum corneum (SC) interface (arrowheads), whereas exocytosis of LBs is still in progress in cKO mice (black arrows). A convoluted interface and lacunae (asterisks) at the SG–SC junction are shown, suggesting that lamellar reorganization is not complete. SG, stratum granulosum. Bars = 200 nm (top panels), 90 nm (bottom panels). Postfixed with RuO_4.

lipid droplets, and extracellular domains largely devoid of lamellae (Ghadially *et al.*, 1996). As the K5 promoter is active in the upper digestive tract as well, hyperkeratosis was also observed in epithelia of the esophagus (data not shown) and the forestomach in SPT-cKO mice, but not in WT mice (Figure 3f, bottom versus top panel). Immunohistological study revealed no SPT expression in the epidermis and the outer root sheath in SPT-cKO, (Figure 3g, left bottom panel), whereas SPT was detected in the epidermis and outer root sheath of WT mice (Figure 3g, left top panel). This was because the conditional gene targeting was undertaken under the K5 promoter. It should be noted that dermal inflammatory cells showed a high SPT expression in SPT-cKO mice (asterisk in Figure 3g).

Activation and enhanced migration of Langerhans cells to lymph nodes in SPT-cKO mice

Staining of epidermal sheets taken from SPT-cKO mice at PD18 with anti-CD207 (langerin) showed that Langerhans cells (LCs) appeared to be somewhat spherical in morphology, with fewer dendrites compared with those of WT mice (Supplementary Figure S6a online). Interestingly, immunostaining with anti-CD207 (langerin) revealed that LCs in SPT-cKO mice had elongated dendrites upward beneath the SC (Supplementary Figure S6b online, right panels), suggesting that LC activation occurred in response to the barrier disruption. In contrast, LCs in WT mice resided in the basal layer of the epidermis with horizontally spreading dendrites (Supplementary Figure S6b online, left bottom panel). Those data support the previous finding that LC activation by TS leads to dendrite elongation that penetrates tight junctions to capture external antigens (Kubo *et al.*, 2009). FACS analysis of isolated LCs from the skin of SPT-cKO mice showed the upregulation of CD80 and CD86 (data not shown), suggesting LC activation. Furthermore, the skin-draining lymph nodes (SDLNs) of SPT-cKO mice showed increased numbers of $CD40^{high}CD11c^{int}$ cells (Supplementary Figure S6c online), suggesting enhanced LC migration from the epidermis (Ruedl *et al.*, 2000). However, there was no increase in numbers of resident DC population identified as $CD40^{int}CD11c^{higt}$ cells (Supplementary Figure S6c online). Staining with anti-langerin of the $CD40^{high}CD11c^{int}$ population revealed large increases in the numbers of $langerin^+$ cells in the SDLNs of SPT-cKO mice compared with WT mice (Supplementary Figure S6d and S6e online). This finding was consistent, in part, with previous reports showing that mechanical disruption of the skin barrier by TS leads to LC activation and migration from the skin to SDLNs (Holzmann *et al.*, 2004; Strid *et al.*, 2011).

Expansion of IL-17-producing γδ T cells in SPT-cKO mice

Quantitative RT–PCR analysis of the skin lesions at PD18 revealed upregulation of psoriatic-associated genes, including Th17 cytokines such as IL-17A, IL-17F, IL-22, S100A8, S100A9, and β-defensins 3 and 4 (Figure 4a). In addition to the histopathological changes, therefore, gene expression profiles of diseased SPT-cKO mice closely resembled psoriasis. As found in the skin lesions, SDLN cells in SPT-cKO mice showed upregulation of mRNA transcript levels of IL-17A, IL-17F, and IL-22 (Figure 4b). FACS analysis of SDLNs from SPT-cKO mice showed that not only IL-17-producing $CD4^+$ cells (Th17) but also $CD4^-CD8^-$ γδ T cells (γδ-17) were increased (Figure 4c and d; data not shown).In addition, there was γδ-17 cell expansion in the skin lesions (Figure 4e). In SPT-cKO mice at PD11, the increase in the number of γδ-17 cells was not evident in SDLNs, and no transcriptional elevation of IL-17A, IL-17F, or IL-22 was found in the skin (Supplementary Figure S7c online, data not shown). At this early age, however, the numbers of migrating DCs including $langerin^+$ cells were increased in SDLNs of SPT-cKO mice (Supplementary Figure S7a and b online). This observation suggests that the migration of LCs from the epidermis precedes the expansion of γδ-17 cells. In the epidermis of SPT-cKO

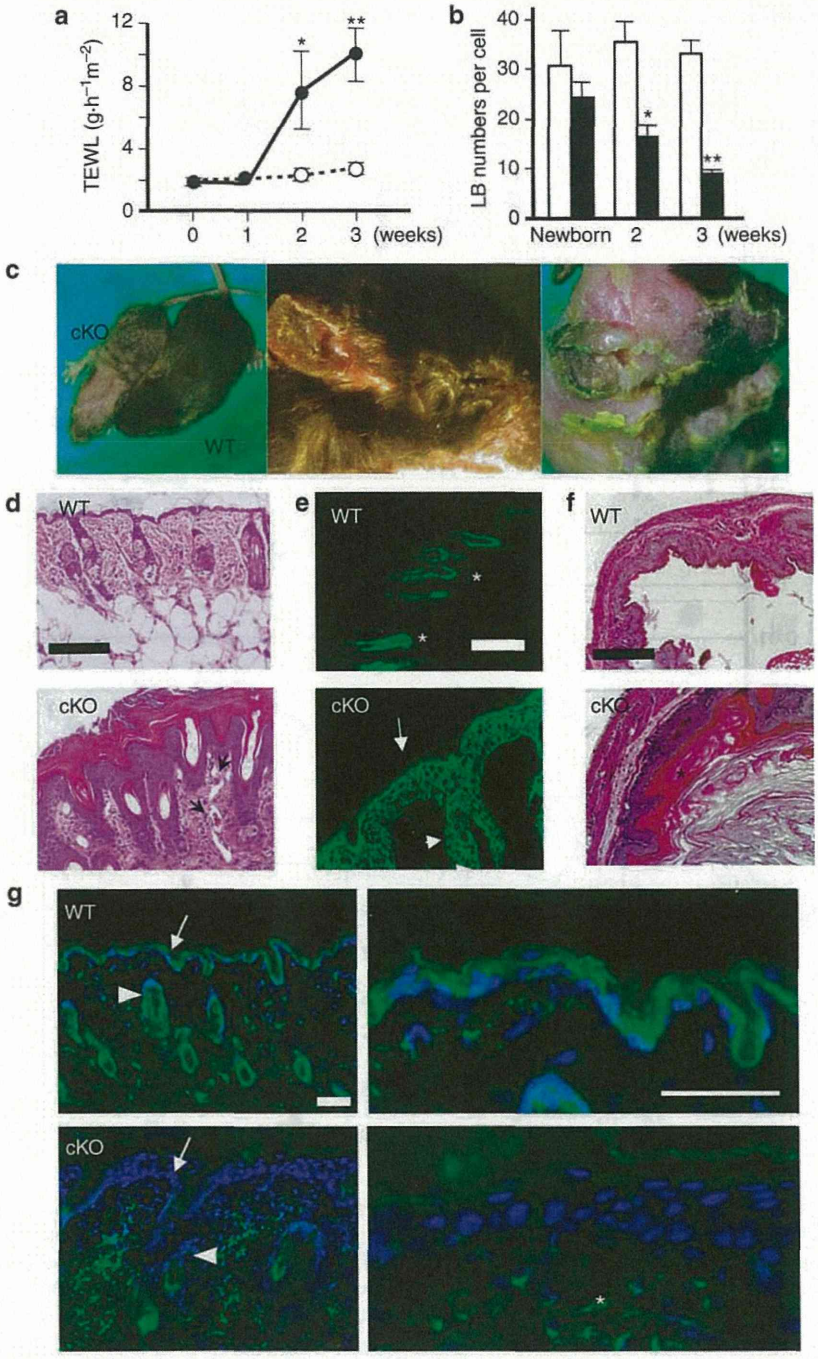

Figure 3. SPT-cKO mice at 2 weeks of age and older develop psoriasis-like skin lesions. (**a**) Barrier disruption developed in SPT-cKO mice from 2 weeks of age and older (solid line, $n=8$), whereas wild-type (WT) mice retained normal barrier function (dotted line, $n=7$). Graphs show transepidermal water loss (mean ± SE). $^{*}P<0.05$. $^{**}P<0.01$. Unpaired Student's *t*-test. (**b**) Decreased numbers of lamellar bodies (LBs) per granular cell in SPT-cKO skin. Using electron micrographs of epidermis postfixed with OsO_4, LB numbers were counted within cells at the granular layer of the epidermis in WT mice (white bars, $n=5$–9) and in SPT-cKO mice (black bars, $n=7$–9) at the indicated age. Graphs show LB numbers per cell (mean ± SE). $^{*}P<0.05$. $^{**}P<0.01$. Unpaired Student's *t*-test. (**c**) SPT-cKO mice at PD14 showed growth retardation and hair loss (left panel). Skin excoriation and scaly lesions developed in the scalp and face at PD18 (middle panel), and severe desquamation and generalized erythema were evident at PD21. Representative mice with a typical phenotype are shown. (**d**) Histological appearance of the dorsal skins in SPT-cKO (bottom) and WT mice (top) at PD19. Marked hyperkeratosis, acanthosis, dermal cell infiltrates, and capillary proliferation (arrows) were noted in SPT-cKO mice. Hematoxylin and eosin (H&E) staining; bar = 100 μm. (**e**) Altered pattern in K6 expression in the back skin of SPT-cKO mice at PD14. In SPT-cKO mice, K6 is expressed ectopically in the interfollicular epidermis (arrow) and in the outer root sheath (arrowhead), within which its expression is confined in WT mice (asterisks). Bar = 100 μm. (**f**) Coincident hyperkeratosis in the forestomach epithelia of SPT-cKO mice at PD19 (bottom, asterisk) compared with WT mice (top). H&E staining. Bar = 200 μm. (**g**) Immunostaining with the anti-SPT antibody of the skin of WT and SPT-cKO (cKO) mice at PD18. Although WT mice are positive for SPT in the epidermis (arrow) and the outer root sheath (arrowhead), SPT-cKO mice are devoid of SPT in the epidermis (arrow) and the outer root sheath (arrowhead). Right panels are high magnifications of left ones. Asterisk, inflammatory cells. Co-stained with 4′,6-diamidino-2-phenylindole. Bars = 50 μm.

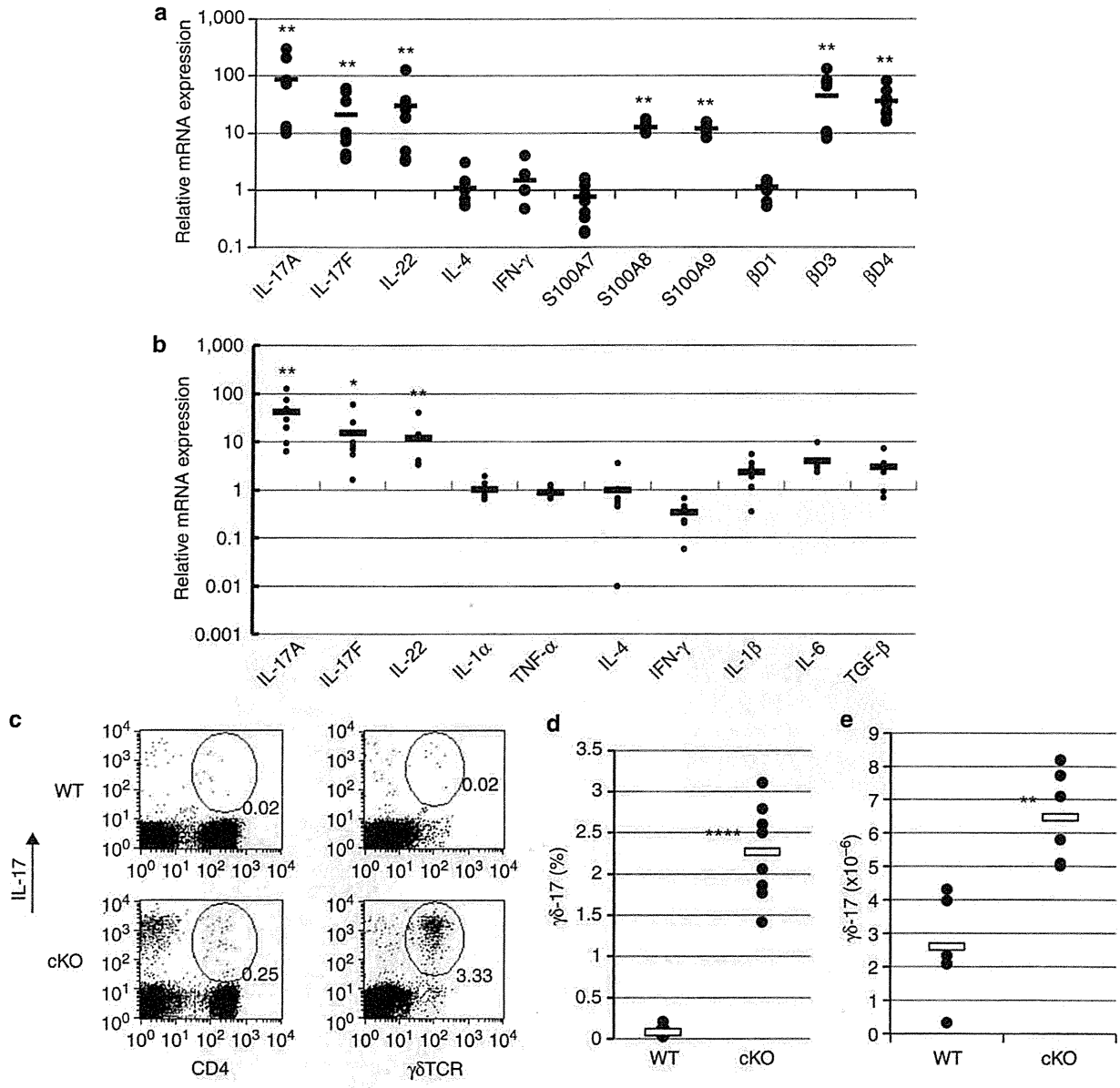

Figure 4. Gene expression profiles of SPT-cKO mice and increased number of IL-17-producing γδ T cells. (**a**) Elevated gene expression of psoriasis-associated molecules such as IL-17A, IL-17F, IL-22, β-defensins (βD), and S100A family members, in the skin lesions of SPT-cKO mice at PD18 ($n=9$) compared with wild-type (WT) skins ($n=7$). mRNA transcript levels of each gene were normalized to HPRT mRNA. Symbols show mean mRNA transcript levels in cKO skin relative to WT skin. $^{**}P<0.01$. Mann–Whitney *U*-test. (**b**) Elevated gene expression of Th17-related cytokines in skin-draining lymph nodes (SDLNs) of SPT-cKO mice at PD18 ($n=8$–11). mRNA transcript levels of each gene were normalized to HPRT mRNA. Symbols show mean mRNA transcript levels in SDLNs from SPT-cKO mice relative to WT mice. $^{*}P<0.05$, $^{**}P<0.01$, Mann–Whitney *U*-test. (**c**) Both IL-17-producing $CD4^+$ cells (Th17) and gd T cells (γδ-17) were increased in SDLN cells from SPT-cKO mice compared with WT mice analyzed by flow cytometry. (**d**) Symbols show mean % of γδ-17 cells in SDLNs from WT ($n=13$) and SPT-cKO ($n=8$) mice. $^{****}P<0.0001$. Unpaired Student's *t*-test. (**e**) There were increased numbers of γδ-17 cells in skin lesions. Symbols show higher γδ-17 cell numbers in the dorsal skin (~2 cm^2 in size) from WT ($n=5$) and SPT-cKO ($n=6$) mice. $^{**}P<0.01$. Unpaired Student's *t*-test.

mice, dendritic epidermal T cells (DETCs) underwent morphological alterations such as a spherical change and a loss of dendrites (Supplementary Figure S8a online), resembling those in LCs (Supplementary Figure S6a online). Coincident rounding of DETCs and LCs was also observed in mouse epidermis after TS, implying that barrier damage provokes the initial events of lymphoid stress surveillance (Strid *et al.*, 2011). However, γδ-17 cells found in SPT-cKO mice were not derived from DETCs, as they did not express Vγ5 (Supplementary Figure S8b online). They are presumably from dermal γδ T cells, which are proinflammatory and mobile (Gray *et al.*, 2011; Sumaria *et al.*, 2011), and also secrete IL-22 as do Th17 cells (Laggner *et al.*, 2011; Mabuchi *et al.*, 2011). In SDLNs, SPT-cKO mice showed increased numbers of IL-22-producing γδ T cells compared with WT mice (Figure 5a). Most γδ T cells in SPT-cKO mice produced both IL-17 and

IL-22, whereas WT mice had a lower percentage of γδ T cells secreting both cytokines (Figure 5b and c). Thus it is likely that barrier disruption in SPT-cKO mice results in activation and proliferation of γδ T cells that produce both IL-17 and IL-22. The thickened epidermis of SPT-cKO mice showed activated Stat3, i.e., they were positive for pY705-Stat3 (Figure 5d), a characteristic of psoriatic epidermis (Sano *et al.*, 2005, 2008). These data also suggest the contribution of IL-22 secreted from skin-infiltrating γδ T cells to acanthosis through Stat3 activation in keratinocytes (Sa *et al.*, 2007; Zheng *et al.*, 2007).

Repeated TS fails to generate psoriasis lesions in WT mice

To assess whether chronic barrier insults would produce a psoriatic phenotype, we performed TS every other day up to four cycles (five strokes of TS per each cycle) onto the back skins of WT mice. Interestingly, the TS-induced TEWL elevation attenuated from the third cycle onward (Supplementary Figure S9a online). This might be due to constitutive upregulation of enzymes for lipid synthesis in response to repeated barrier insults. Histologically, repeated TS did not induce epidermal hyperplasia or detectable inflammation (Supplementary Figure S9b online). Quantitative RT–PCR using the treated skins did not detect significant gene signatures, including IL-17A, IL-17F, IL-22, BD3, BD4, and S100A8/9, all of which were increased in SPT-cKO mice (Supplementary Figure S9c online). However, K5.Stat3C transgenic mice, in which keratinocytes express the activation-prone Stat3 (Sano *et al.*, 2005), showed persistent barrier disruption by TS and developed psoriasis-like skin lesions where a number of IL-22-producing cells infiltrated in the dermis (Supplementary Figure S10 online). These results suggest that persistent barrier disruption either by ceramide deficiency or the intrinsic signal abnormality within keratinocytes contributes to the development of a psoriasis-like phenotype.

IL-23 stimulation is required for the expansion of γδ-17 cells and psoriasis-like lesions

In the inflamed skin, the upregulation of IL-23p19 and IL-12/23p40 mRNA transcripts was observed, whereas IL-12p35 mRNA transcripts were unchanged compared with WT mice (Figure 6a). These data suggest the predominant involvement of IL-23 over IL-12 in skin lesions of SPT-cKO mice. The profile tendencies of these genes in SPT-cKO mice are similar to those in human psoriasis and in K5.Stat3C mice (Nakajima *et al.*, 2011). Immunostaining of skin lesions displayed an enriched accumulation of IL-23$^+$CD11c$^+$ cells in the dermis (Figure 6b). IL-23 stimulates the survival and proliferation of Th17 cells, and critically participates in the pathogenesis of psoriasis (Fitch *et al.*, 2007; Nakajima *et al.*, 2011). Therefore, targeting IL-23 leads to clinical improvement in psoriatic patients (Nograles and Krueger, 2011). Treatment of SPT-cKO mice with an anti-IL-12/23p40 antibody greatly attenuated the skin inflammation and epidermal hyperplasia (Figure 6c and d). At the same time, the numbers of γδ-17 cells in SDLNs were decreased (Figure 6e). This implicates a role for IL-23 in the expansion of disease-associated γδ-17 cells.

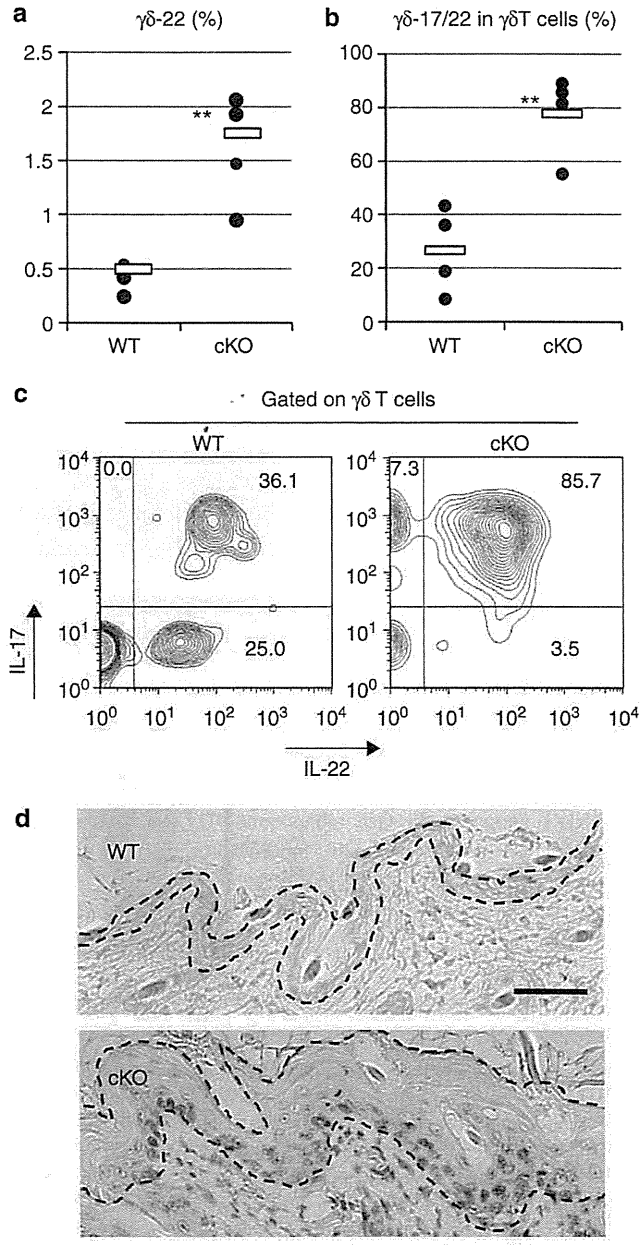

Figure 5. Most γδ-17 cells produce IL-22, and thickened epidermis shows Stat3 activation in SPT-cKO mice. (**a**) There were increased numbers of IL-22-producing γδ T cells (γδ-22) in skin-draining lymph nodes (SDLNs) from SPT-cKO mice at PD18 ($n=4$) compared with wild-type (WT) ($n=4$) mice. $^{**}P<0.01$. Unpaired Student's *t*-test. (**b**) Most of the γδ T cells produced both IL-17 and IL-22 in SDLNs from SPT-cKO mice ($n=4$), whereas a lower % of them produced both cytokines in WT mice ($n=4$). Symbols show mean % of γδ-17/22 cells within γδ T cells. $^{**}P<0.01$. Unpaired Student's *t*-test. (**c**) Representative flow cytometric data of SDLN cells gated on γδ T cells. (**d**) Immunohistochemical staining with anti-phosphorylated (pY) Stat3 (Y705) of WT and SPT-cKO mice at PD18. Representative micrographs are shown from three independent experiments. The thickened epidermis of SPT-cKO mice showed pY-Stat3 in epidermal cells, in particular at the basal layer, whereas no pY-Stat3 was detected in the epidermis of WT mice. Dotted lines, epidermis. Bar = 50 μm.

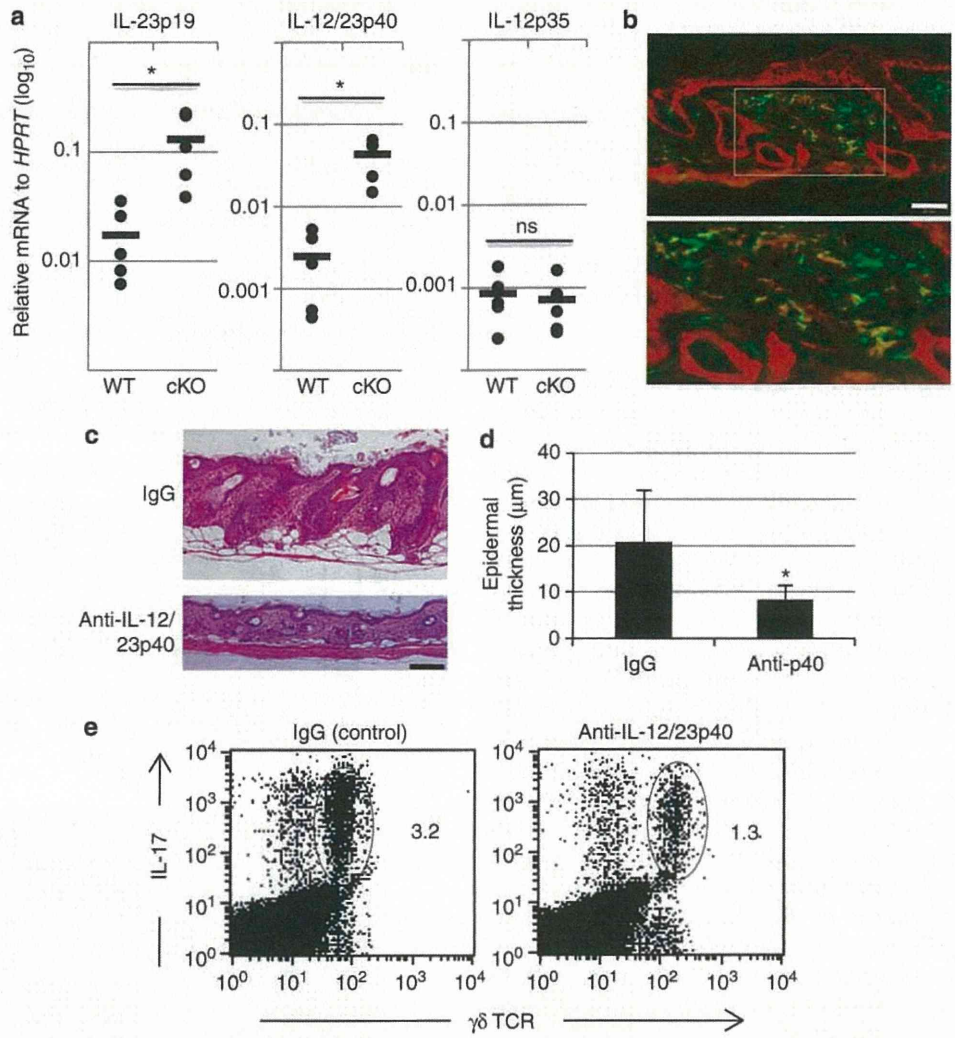

Figure 6. Involvement of IL-23 in the generation of skin lesions in SPT-cKO mice. (**a**) Upregulated mRNA transcript levels of IL-23 in skin lesions of SPT-cKO mice at PD18 ($n=5$) compared with skins of wild-type (WT) mice ($n=5$). Symbols show mean mRNA transcript levels. *$P<0.05$. ns, not significant. Unpaired Student's *t*-test. (**b**) Accumulation of IL-23$^+$CD11c$^+$ cells in the dermis of skin lesions of SPT-cKO mice at PD18. Immunostaining with anti-IL-23p19 (red) and anti-CD11c (green) antibodies. Bottom panel shows a high magnification view of the rectangular area in the top panel. Note that the epidermis also expresses IL-23p19. Bar = 50 μm. (**c**) Intraperitoneal administration of anti-IL-12/23p40 antibody to SPT-cKO mice attenuated the skin lesions (hematoxylin and eosin). Bar = 100 μm. Representative histology is shown from three independent experiments. (**d**) Attenuation of epidermal hyperplasia by anti-IL-12/23p40 treatment. Bars show epidermal thickness (mean μm ± SD) of skin lesions of SPT-cKO mice treated with control IgG ($n=3$) or with anti-IL-12/23p40 ($n=6$). *$P<0.05$. Unpaired Student's *t*-test. (**e**) Decline in numbers of γδ-17 cells in skin-draining lymph nodes after treatment with anti-IL-12/23p40 compared with those treated with IgG control. Representative data are shown from three independent experiments.

DISCUSSION

Epithelial-specific genes have been identified as candidates of psoriasis susceptibility, including corneodesmosin (*CDSN*) gene (Orru *et al.*, 2005), the β-defensin cluster (Hollox *et al.*, 2008), and late cornified envelope (LCE) 3B and 3C genes (*LCE3C_LCE3B*-del) (de Cid *et al.*, 2009). Barrier dysfunction is a putative contribution of these genes in psoriasis (Roberson and Bowcock, 2010). This view may change the paradigm of the etiology of psoriasis, like AD in which loss-of-mutation of *FLG* was identified (Palmer *et al.*, 2006).

Ceramides in the SC are essential for barrier homeostasis, and its downside has been observed in lesional skin of psoriasis, as well as AD (Melnik *et al.*, 1988; Holleran *et al.*, 1991; Imokawa *et al.*, 1991; Motta *et al.*, 1993, 1994; Alessandrini *et al.*, 2004). SPT expression was reported to be significantly reduced in psoriatic lesions compared with psoriatic uninvolved skins and inversely correlated with Psoriasis Area Severity Index (PASI) score (Hong *et al.*, 2007). In another study, alterations of sphingomyelidase levels were observed in psoriatic lesions (Alessandrini *et al.*, 2004). Therefore, ceramide deficiency and resulting barrier disruption may be crucial for the development of psoriasis (Wolf *et al.*, 2012).

In the present study, newly established keratinocyte-specific SPT-cKO mice have suggested the profound interactions

between barrier dysfunction and immunological alterations that lead to psoriasis phenotype. Repeated barrier insults by TS did not upregulate psoriasis-associated gene expressions or produce psoriasis-like lesions in WT mice. This result suggests that ceramide deficiency, but not barrier abnormality alone, contributes to the development of a psoriatic phenotype in SPT-cKO mice. However, it should be noted that psoriasis-like inflammation could be induced by chronic barrier disruption due to essential fatty acid deficiency (Wood *et al.*, 1994, 1997; Jansen *et al.*, 2002). K5.Stat3C mice, which represent psoriasis model mice (Sano *et al.*, 2005), showed persistent barrier disruption by TS and at the same time developed psoriasis-like lesions with a number of IL-22-producing T cells in the dermis, similar to SPT-cKO mice. As ceramide deficiency led to psoriasis-like lesions, topical ceramides may improve barrier function, the immunological abnormalities, and psoriatic skin phenotype.

As γδ-17 cells are not derived from DETCs, we assume that they are dermal γδ T cells, which are thought to be a major subset of IL-17-precommitted cells in mouse skin (Gray *et al.*, 2011), and play a role in the innate immunity against infection and in development of the psoriasis-like dermatitis (Mabuchi *et al.*, 2011). The importance of IL-23 is supported by data showing that IL-23p19 and IL-12/23p40 mRNA levels were increased in the lesions, and the treatment with anti-IL-12/23 antibody reduced γδ-17 cells numbers and attenuated lesions. In intradermal IL-23 treatment or topical imiquimod treatment models, γδ-17 cells were associated with psoriasis-like phenotype (Cai *et al.*, 2011; Mabuchi *et al.*, 2011). Imiquimod-induced skin inflammation and epidermal hyperplasia were significantly attenuated in *Tcrd*$^{-/-}$ mice (Cai *et al.*, 2011). In psoriasis patients, both Th17 cells and γδ-17 cells were found to be the IL-23-responsive IL-17 producers (Cai *et al.*, 2011; Laggner *et al.*, 2011).

The causal relationship between the epidermal dysfunction and immunological abnormalites including LCs, γδ-17 cells, and Th17 cells needs to be clarified to understand the pathogenesis of psoriasis.

MATERIALS AND METHODS

Mice

All animal studies were approved by Institutional Animal Care and Use Committees at Osaka University and Kochi University. Cre-mediated *sptlc2* gene–targeted mice were generated by crossing floxed *sptlc2* mice (Ohta *et al.*, 2009) with K5-Cre transgenic mice (Tarutani *et al.*, 1997).

Patients and normal controls

The study protocol was conducted in accordance with the guidelines of the World Medical Association's Declaration of Helsinki and was approved by the Institute Ethical Review Board of the Kochi Medical School, Kochi University. Nine patients with chronic, plaque-type psoriasis (6 male and 3 female individuals) were recruited from the Department of Dermatology, Kochi Medical School Hospital in Nankoku, Kochi, Japan. Normal control skin was obtained from nine healthy volunteers (five male and four female individuals). We obtained written informed consents from all the patients and healthy volunteers.

In vivo administration of antibodies

Details of anti-IL-12/23p40 (CNTO 3913) and control IgG (CNTO 1322) were described (Nakajima *et al.*, 2011). Antibodies at a dose of 300 μg per mouse were administered intraperitoneally at PD6. Skin and SDLN node cells were sampled at PD18.

Immunohistochemical staining

Antibodies used included: anti-ceramides (ENZO Life Science, Farmingdale, NY), anti-CD3ε (Santa Cruz Biotechnology, Santa Cruz, CA), anti-IL-23p19 (ab45420, Abcam, Cambridge, England), anti-IL-22 (Novus Biologicals, Littleton, CO), anti-CD11c (BioLegend, San Diego, CA), anti-CD207 (eBioscience, San Diego, CA), anti-TCR γδ (Santa Cruz Biotechnology), anti-Gr-1 (R&D systems, Minneapolis, MN), anti-SPT (Abcam), anti-keratin 1, 5, 6, involucrin, filaggrin, and loricrin (Covance, Princeton, NJ). Staining was performed on either formalin-fixed paraffin-embedded, snap-frozen sections, or epidermal sheets using relevant secondary antibodies as described (Nakajima *et al.*, 2011).

Flow cytometric analysis

All the antibodies used were conjugated with fluorochrome. Intracellular staining with anti-IL-17 (BioLegend) and anti-IL-22 (R&D Systems) was performed as described (Nakajima *et al.*, 2011). To identify DETCs, anti-Vγ5 (BD Pharmingen, San Diego, CA) and anti-TCR-γδ (BioLegend) were used. Langerin^{+} cells were stained with anti-CD40 and CD11c (BD Pharmingen), followed by permeabilization, and treated with biotin-labeled anti-CD207 (eBioscience) and FITC-streptavidin (BD Pharmingen). Cells were analyzed using a FACSCalibur (BD Biosciences, San Jose, CA) or a JSAN (Bay Bioscience, Kobe, Japan) and were then analyzed with CellQuest Pro software (BD Biosciences) or FlowJo software (Treestar, Ashland, OR).

Imaging mass spectrometric (IMS) analyses

The protocol of IMS was previously described elsewhere (Goto-Inoue *et al.*, 2012).

Determination of TEWL and SC hydration

To evaluate TEWL, we used a Tewameter (TEWAMETER TM300, Courage & Khazaka, Cologne, Germany) from six separate sites per mouse. For analyses of SC hydration, a skin-surface hygrometer (Skicon-200, IBS, Hamamatsu, Japan) was used. The measurements were repeated at least six times to obtain averages.

Electron microscopy

Mouse skins were fixed overnight in cacodylate-buffered 2.0% glutaraldehyde and then post-fixed in both 1% aqueous osmium tetroxide (OsO_4) and 0.5% aqueous ruthenium tetroxide (RuO_4) containing 0.25% potassium ferrocyanide, then embedded in Quetol 812. Thin sections were stained with uranyl acetate and lead citrate and examined with a JEOL JEM-1010 transmission electron microscope (JEOL, Tokyo, Japan) in transmission mode at 80 kV.

Quantitative (q) RT–PCR

Dorsal skin and SDLN cells from mice were minced with scissors into small pieces on ice, and were then disrupted by ultrasonic sonication. Extraction of RNA and qRT–PCR were performed as described (Nakajima *et al.*, 2011).

Statistical analysis

All samples were compared with two-tailed, unpaired Student's *t*-test, Wilcoxon *t*-test, or Mann–Whitney *U*-test as indicated. *P*-values less than 0.05 are considered significant.

CONFLICT OF INTEREST

The authors state no conflict of interest.

ACKNOWLEDGMENTS

We thank Sou Osuka and Yoshio Hirabayashi for kindly providing the floxed *sptlc2* mice and Centocor Research & Development for generously providing rat/mouse anti-mouse IL-12/23p40 (CNTO 3913) and rat/mouse chimeric mouse IgG control (CNTO 1322); Kim Campbell, Yoshikazu Uchida, Walter M. Holleran, and Peter M. Elias for helpful discussion; Tomoko Nagayama and Reiko Kamijima for technical assistance; and Dr Hideki Nakajima for help with statistical analyses. This work was partly supported by Grants-in-Aid for Scientific Research from the Ministry of Education, Culture, Sports, Science and Technology of Japan (21591436, 21591467, 21591656) and by a fund subsidy of "Research on Measures for Intractable Diseases" from the Ministry of Health, Labour, and Welfare of Japan (H23-028), and by grants from the Center of Biomembrane Functions Controlling Biological Systems of the Kochi University Research Center Project.

SUPPLEMENTARY MATERIAL

Supplementary material is linked to the online version of the paper at http://www.nature.com/jid

REFERENCES

Alessandrini F, Pfister S, Kremmer E *et al.* (2004) Alterations of glucosylceramide-beta-glucosidase levels in the skin of patients with psoriasis vulgaris. *J Invest Dermatol* 123:1030–6

Bergboer JG, Zeeuwen PL, Schalkwijk J (2012) Genetics of psoriasis: evidence for epistatic interaction between skin barrier abnormalities and immune deviation. *J Invest Dermatol* 132:2320–1

Cai Y, Shen X, Ding C *et al.* (2011) Pivotal role of dermal IL-17-producing gammadelta T cells in skin inflammation. *Immunity* 35:596–610

de Cid R, Riveira-Munoz E, Zeeuwen PL *et al.* (2009) Deletion of the late cornified envelope LCE3B and LCE3C genes as a susceptibility factor for psoriasis. *Nat Genet* 41:211–5

Dickson RC, Lester RL, Nagiec MM (2000) Serine palmitoyltransferase. *Methods Enzymol* 311:3–9

Elias PM, Menon GK (1991) Structural and lipid biochemical correlates of the epidermal permeability barrier. *Adv Lipid Res* 24:1–26

Feingold KR (2007) Thematic review series: skin lipids. The role of epidermal lipids in cutaneous permeability barrier homeostasis. *J Lipid Res* 48:2531–46

Fitch E, Harper E, Skorcheva I *et al.* (2007) Pathophysiology of psoriasis: recent advances on IL-23 and Th17 cytokines. *Curr Rheumatol Rep* 9:461–7

Ghadially R, Reed JT, Elias PM (1996) Stratum corneum structure and function correlates with phenotype in psoriasis. *J Invest Dermatol* 107:558–64

Goto-Inoue N, Hayasaka T, Zaima N *et al.* (2012) Imaging mass spectrometry visualizes ceramides and pathogenesis of dorfman-chanarin syndrome due to ceramide metabolic abnormality in the skin. *PLOS ONE* 7:e49519

Gray EE, Suzuki K, Cyster JG (2011) Cutting edge: identification of a motile IL-17-producing gammadelta T cell population in the dermis. *J Immunol* 186:6091–5

Hwang J, Kita R, Kwon H-S *et al.* (2012) Epidermal ablation of Dlx3 is linked to IL-17-associated skin inflammation. *Proc Natl Acad Sci USA* 108:11566–71

Holleran WM, Feingold KR, Man MQ *et al.* (1991) Regulation of epidermal sphingolipid synthesis by permeability barrier function. *J Lipid Res* 32:1151–8

Holleran WM, Gao WN, Feingold KR *et al.* (1995) Localization of epidermal sphingolipid synthesis and serine palmitoyl transferase activity: alterations imposed by permeability barrier requirements. *Arch Dermatol Res* 287:254–8

Holleran WM, Williams ML, Gao WN *et al.* (1990) Serine-palmitoyl transferase activity in cultured human keratinocytes. *J Lipid Res* 31:1655–61

Hollox EJ, Huffmeier U, Zeeuwen PL *et al.* (2008) Psoriasis is associated with increased beta-defensin genomic copy number. *Nat Genet* 40:23–5

Holzmann S, Tripp CH, Schmuth M *et al.* (2004) A model system using tape stripping for characterization of Langerhans cell-precursors in vivo. *J Invest Dermatol* 122:1165–74

Hong KK, Cho HR, Ju WC *et al.* (2007) A study on altered expression of serine palmitoyltransferase and ceramidase in psoriatic skin lesion. *J Korean Med Sci* 22:862–7

Imokawa G, Abe A, Jin K *et al.* (1991) Decreased level of ceramides in stratum corneum of atopic dermatitis: an etiologic factor in atopic dry skin? *J Invest Dermatol* 96:523–6

Irvine AD, McLean WH, Leung DY (2011) Filaggrin mutations associated with skin and allergic diseases. *N Engl J Med* 365:1315–27

Jansen M, Groth L, Holmer G *et al.* (2002) The potential of the essential fatty acid-deficient hairless rat as a psoriasis screening model for topical anti-proliferative drugs. *Skin Pharmacol Appl Skin Physiol* 15:401–13

Kubo A, Nagao K, Yokouchi M *et al.* (2009) External antigen uptake by Langerhans cells with reorganization of epidermal tight junction barriers. *J Exp Med* 206:2937–46

Laggner U, Di Meglio P, Perera GK *et al.* (2011) Identification of a novel proinflammatory human skin-homing Vgamma9Vdelta2 T cell subset with a potential role in psoriasis. *J Immunol* 187:2783–93

Mabuchi T, Takekoshi T, Hwang ST (2011) Epidermal CCR6+ gammadelta T cells are major producers of IL-22 and IL-17 in a murine model of psoriasiform dermatitis. *J Immunol* 187:5026–31

Melnik B, Hollmann J, Plewig G (1988) Decreased stratum corneum ceramides in atopic individuals–a pathobiochemical factor in xerosis? *Br J Dermatol* 119:547–9

Motta S, Monti M, Sesana S *et al.* (1993) Ceramide composition of the psoriatic scale. *Biochim Biophys Acta* 1182:147–51

Motta S, Monti M, Sesana S *et al.* (1994) Abnormality of water barrier function in psoriasis. Role of ceramide fractions. *Arch Dermatol* 130:452–6

Nakajima K (2012) Critical role of the interleukin-23/T-helper 17 cell axis in the pathogenesis of psoriasis. *J Dermatol* 39:219–24

Nakajima K, Kanda T, Takaishi M *et al.* (2011) Distinct roles of IL-23 and IL-17 in the development of psoriasis-like lesions in a mouse model. *J Immunol* 186:4481–9

Nograles KE, Krueger JG (2011) Anti-cytokine therapies for psoriasis. *Exp Cell Res* 317:1293–300

Ohta E, Ohira T, Matsue K *et al.* (2009) Analysis of development of lesions in mice with serine palmitoyltransferase (SPT) deficiency -Sptlc2 conditional knockout mice. *Exp Anim* 58:515–24

Orru S, Giuressi E, Carcassi C *et al.* (2005) Mapping of the major psoriasis-susceptibility locus (PSORS1) in a 70-Kb interval around the corneodesmosin gene (CDSN). *Am J Hum Genet* 76:164–71

Palmer CN, Irvine AD, Terron-Kwiatkowski A *et al.* (2006) Common loss-of-function variants of the epidermal barrier protein filaggrin are a major predisposing factor for atopic dermatitis. *Nat Genet* 38:441–6

Roberson ED, Bowcock AM (2010) Psoriasis genetics: breaking the barrier. *Trends Genet* 26:415–23

Ruedl C, Koebel P, Bachmann M *et al.* (2000) Anatomical origin of dendritic cells determines their life span in peripheral lymph nodes. *J Immunol* 165:4910–6

Sa SM, Valdez PA, Wu J *et al.* (2007) The effects of IL-20 subfamily cytokines on reconstituted human epidermis suggest potential roles in cutaneous innate defense and pathogenic adaptive immunity in psoriasis. *J Immunol* 178:2229–40

Sano S, Chan KS, Carbajal S *et al.* (2005) Stat3 links activated keratinocytes and immunocytes required for development of psoriasis in a novel transgenic mouse model. *Nat Med* 11:43–9

Sano S, Chan KS, DiGiovanni J (2008) Impact of Stat3 activation upon skin biology: a dichotomy of its role between homeostasis and diseases. *J Dermatol Sci* 50:1–14

Strid J, Sobolev O, Zafirova B *et al.* (2011) The intraepithelial T cell response to NKG2D-ligands links lymphoid stress surveillance to atopy. *Science* 334:1293–7

Sumaria N, Roediger B, Ng LG *et al.* (2011) Cutaneous immunosurveillance by self-renewing dermal gammadelta T cells. *J Exp Med* 208:505–18

Tarutani M, Itami S, Okabe M *et al.* (1997) Tissue-specific knockout of the mouse Pig-a gene reveals important roles for GPI-anchored proteins in skin development. *Proc Natl Acad Sci USA* 94:7400–5

Wood LC, Jackson SM, Elias PM *et al.* (1992) Cutaneous barrier perturbation stimulates cytokine production in the epidermis of mice. *J Clin Invest* 90:482–7

Wood LC, Elias PM, Sequeira-Martin SM *et al.* (1994) Occlusion lowers cytokine mRNA levels in essential fatty acid-deficient and normal mouse epidermis, but not after acute barrier disruption. *J Invest Dermatol* 103:834–8

Wood LC, Stalder AK, Liou A *et al.* (1997) Barrier disruption increases gene expression of cytokines and the 55kD TNF receptor in murine skin. *Exp Dermatol* 6:98–104

Wolf R, Orion E, Ruocco E *et al.* (2012) Abnormal epidermal barrier in the pathogenesis of psoriasis. *Clin Dermatol* 30:323–8

Zheng Y, Danilenko DM, Valdez P *et al.* (2007) Interleukin-22, a T(H)17 cytokine, mediates IL-23-induced dermal inflammation and acanthosis. *Nature* 445:648–51

α(1,3) Fucosyltransferases IV and VII Are Essential for the Initial Recruitment of Basophils in Chronic Allergic Inflammation

Kazumi Saeki[1], Takahiro Satoh[2] and Hiroo Yokozeki[1]

Basophils act as initiator cells for the development of IgE-mediated chronic allergic inflammation (IgE-CAI). However, detailed mechanisms of initial recruitment of basophils into the skin have yet to be clarified. Selectins mediate leukocyte capture and rolling on the vascular endothelium for extravasation. Counter-receptor activity of selectins is regulated by α(1, 3) fucosyltransferases (FTs) IV and VII. To clarify the contribution of selectin ligands regulated by FTs for initial basophil recruitment, IgE-CAI was induced in mice deficient in *FT-IV* and/or *FT-VII* genes. Although FT-IV(−/−) and FT-VII(−/−) mice exhibited comparable skin responses to wild-type mice, the FT-IV(−/−)/FT-VII(−/−) mice showed significantly impaired inflammation. Although the transfer of basophils to FcRγ(−/−) mice induced IgE-CAI, this induction was completely absent when basophils from FT-IV(−/−)/FT-VII(−/−) mice were transferred. L-selectin, but not P- and E-selectin, blocking Abs inhibited skin inflammation *in vivo*. P-selectin glycoprotein-1 (PSGL-1) antibody also ameliorated skin inflammation, and basophils were bound to L-selectin in a PSGL-1-dependent manner, which was regulated by FT-IV/VII. Functional PSGL-1 generated by basophil FT-IV/VII and its subsequent binding to L-selectin could be one of the essential steps required for initial basophil recruitment and the development of IgE-CAI in mice.

Journal of Investigative Dermatology advance online publication, 9 May 2013; doi:10.1038/jid.2013.160

INTRODUCTION

Leukocyte recruitment from the vasculature to the inflammatory sites is a multistep process. The first step of extravasation is leukocyte capture and rolling along the endothelial surfaces, a process that is mediated by selectins. P- and E-selectins on the endothelial cells contribute to the primary capture of leukocytes via binding to their ligands. Conversely, L-selectin is constitutively expressed on most types of circulating leukocytes. L-selectin binds to its ligands on activated endothelial cells (Spertini *et al.*, 1992; Luscinskas *et al.*, 1994; Tu *et al.*, 1999), and also mediates binding to leukocytes already adhering to endothelial cells (secondary capture) (Guyer *et al.*, 1996; Walcheck *et al.*, 1996).

The glycans that contribute to selectin counter-receptor activity arise through glycosylation reactions in which the terminal steps are catalyzed by α(1,3) fucosyltransferases (FTs) (Lowe, 2002). Mice deficient in the *FT-VII* gene (FT-VII(−/−) mice) are characterized by absent P-, E-, and L-selectin ligand activities (Maly *et al.*, 1996). Although the contribution of FT-IV is somewhat subtle when FT-VII is expressed (Weninger *et al.*, 2000), the inflammation-dependent leukocyte recruitment is retained in the FT-VII(−/−) mice. However, it is extinguished in the FT-IV(−/−)/FT-VII(−/−) mice, indicating that FT-IV contributes to E-, P-, and L-selectin ligand generation (Homeister *et al.*, 2001).

Basophils represent <1% of the peripheral blood leukocytes. Under physiological conditions, basophils do not reside in the peripheral tissues. However, basophils can infiltrate into the skin during inflammatory conditions (Ito *et al.*, 2011). Despite the similarities of basophils and mast cells, recent studies have revealed unique functions for basophils, such as producing IL-4 and IL-13 (Redrup *et al.*, 1998; Sokol *et al.*, 2008; Watanabe *et al.*, 2008), and functioning as antigen-presenting cells that induce Th2 cells (Sokol *et al.*, 2009). Basophils also mediate protective immunity against helminthes and ticks (Voehringer, 2009; Wada *et al.*, 2010), in addition to being indispensable for IgG-mediated anaphylactic reactions in mice (Tsujimura *et al.*, 2008).

IgE-mediated chronic allergic inflammation (IgE-CAI) is a long-lasting inflammation that follows immediate-type reactions and late-phase responses. It is histopathologically characterized by numerous eosinophils and mast cells (Mukai *et al.*, 2005; Obata *et al.*, 2007). Although tissue basophils constitute only a minor population of total cellular infiltrate, they have a critical role in the development of IgE-CAI. After a depletion of basophils but not the mast cells, it has been

[1]*Department of Dermatology, Tokyo Medical and Dental University, Tokyo, Japan and* [2]*Department of Dermatology, National Defense Medical College, Tokorozawa, Japan*

Correspondence: Takahiro Satoh, Department of Dermatology, National Defense Medical College, 3-2 Namiki, Tokyo, Tokorozawa 359-8513, Japan. E-mail: tasaderm@ndmc.ac.jp

Abbreviations: CHS, contact hypersensitivity; FT, α(1, 3) fucosyltransferase; IgE-CAI, IgE-mediated chronic allergic inflammation; mRNA, messenger RNA; PSGL-1, P-selectin glycoprotein-1; TNP, trinitrophenyl; WT, wild type

Received 30 August 2012; revised 11 February 2013; accepted 11 March 2013; accepted article preview online 3 April 2013

shown that there is an almost complete abrogation of IgE-CAI (Obata *et al.*, 2007). Thus, basophils are now considered to initiate inflammation of IgE-CAI. Nevertheless, the current understanding of early events involving basophil recruitment to the skin remains limited. This study was designed to determine the requirements of selectin ligand activity for initial basophil recruitment to the skin controlled by FT-IV and -VII during IgE-CAI.

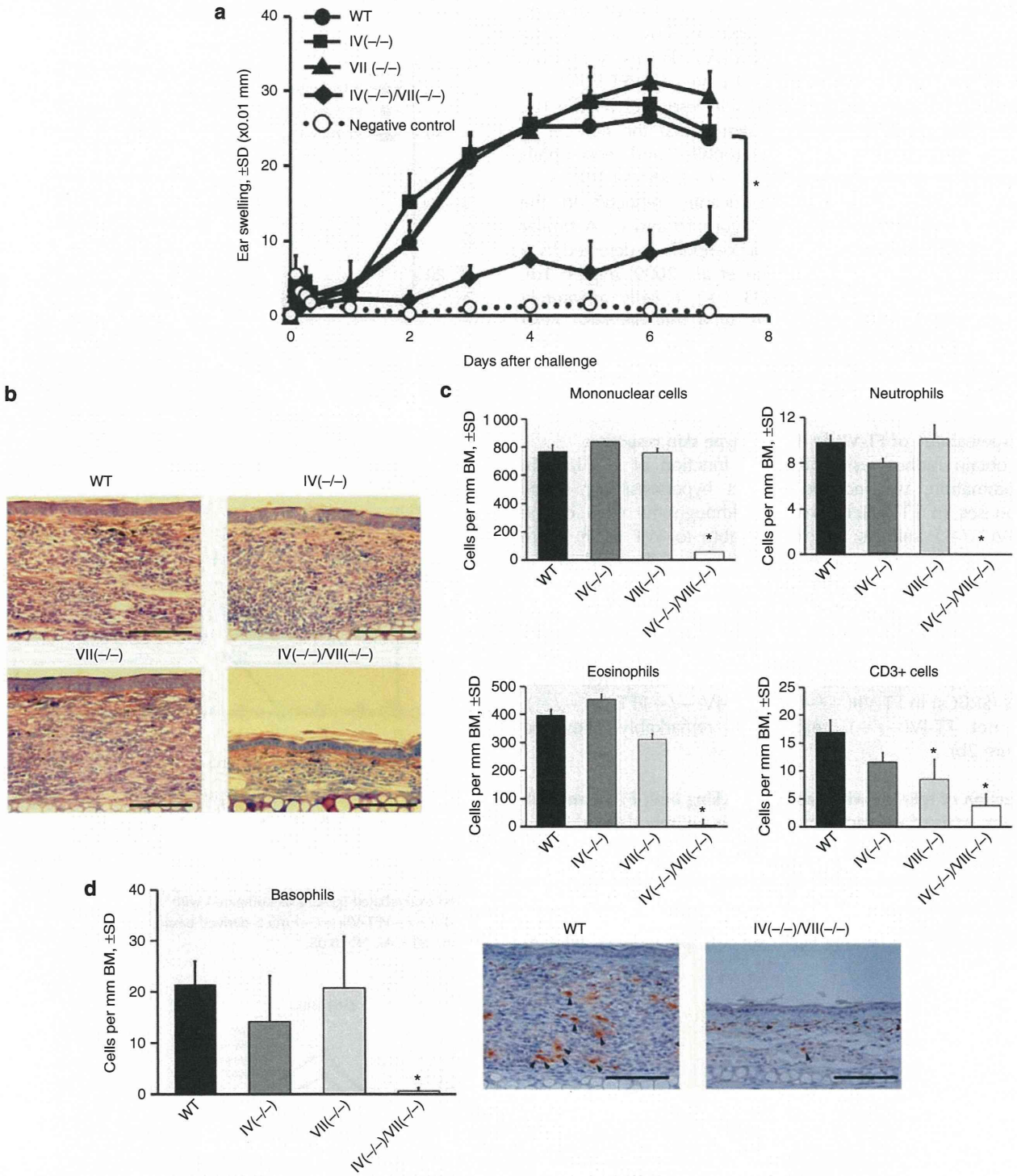

Figure 1. IgE-mediated chronic allergic inflammation (IgE-CAI) in α(1, 3) fucosyltransferase-IV (FT-IV)- and/or FT-VII-deficient mice. (**a**) IgE-CAI was induced in mice lacking FT-IV and/or FT-VII. Negative control mice were challenged with trinitrophenyl-OVA (TNP-OVA) without TNP-IgE injection. (**b**) Histopathological features of the skin (Giemsa's staining). (**c**) Cell populations in inflammatory skin. (**d**) Basophil numbers in inflammatory skin. Basophils were detected by mouse mast cell protease-8 mAb (arrows in the right panel). *$P<0.05$ compared with wild-type (WT) mice. BM, basement membrane. Bar = 100 μm.

RESULTS

Dependency of IgE-CAI on the collaborative functions of FT-IV and FT-VII

To determine selectins and FTs contribution to skin inflammation, IgE-CAI was induced in FT-IV(−/−), FT-VII(−/−), and FT-IV(−/−)/FT-VII(−/−) mice. FT-IV(−/−) mice exhibited levels of skin responses comparable to those seen in the wild-type (WT) mice. In addition, FT-VII deficiency also did not affect IgE-CAI. Nevertheless, FT-IV(−/−)/FT-VII(−/−) mice showed remarkably reduced skin responses (Figure 1a). Histological examination demonstrated that the number of dermal mononuclear cells, neutrophils, and eosinophils were similar among the WT, FT-IV(−/−), and FT-VII(−/−) mice, although they were significantly reduced in the FT-IV(−/−)/FT-VII(−/−) mice (Figure 1b and c). A similar trend was noted for the number of basophils as detected by a basophil-specific antibody (Ugajin *et al.*, 2009) (Figure 1d). Conversely, the number of CD3 (+) T cells apparently decreased in FT-VII(−/−) mice, with this decrease even more prominent in FT-IV(−/−)/FT-VII(−/−) mice (Figure 1c). These findings demonstrate that IgE-CAI is dependent on both FT-IV and FT-VII.

Indispensability of FT-VII in delayed-type skin responses

To obtain further insight into the function of FTs in skin inflammation, we induced contact hypersensitivity (CHS) responses in FT-deficient mice. Although the CHS of the FT-IV(−/−) animals was comparable to WT mice, there was a significantly reduced skin response observed in FT-VII(−/−) mice, unlike that seen for IgE-CAI. Consistent with a previous report (Smithson *et al.*, 2001), CHS was almost completely absent in FT-IV(−/−)/FT-VII(−/−) mice (Figure 2a). Similarly, as compared with the WT mice, delayed-type hypersensitivity reactions to sheep red blood cells (SRBCs) in FT-VII(−/−) and FT-IV(−/−)/FT-VII(−/−), but not FT-IV(−/−), mice were remarkably alleviated (Figure 2b).

Induction of IgE-CAI with basophils lacking both FT-IV and VII

On the basis of the fact that IgE-CAI is entirely dependent on basophils (Mukai *et al.*, 2005; Obata *et al.*, 2007), we attempted to determine the contribution of selectin ligands generated by basophil FTs to the development of skin responses. Basophil transfer from WT mice to irradiated FcRγ(−/−) mice lacking FcεRI successfully induced IgE-CAI (Figure 3a), which was consistent with a prior report (Mukai *et al.*, 2005). Basophil-enriched cell suspension consisted of ~20% primary basophils and ~80% other cells, including CD49b (+) natural killer (NK) cells. Nevertheless, NK cells, T cells, NKT cells, B cells, and

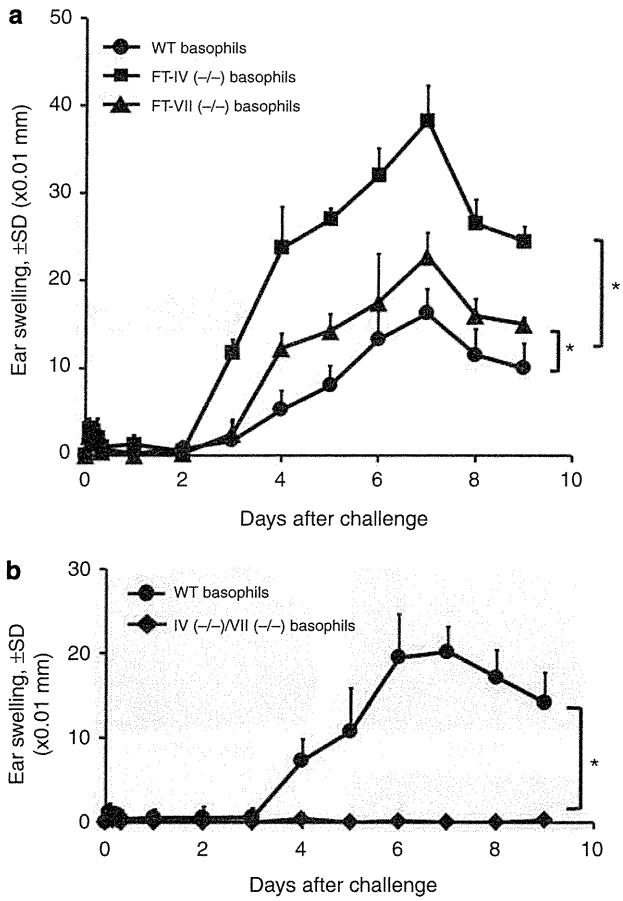

Figure 3. α(1, 3) Fucosyltransferase-IV/VII (FT-IV/VII) in basophils are indispensable for IgE-mediated chronic allergic inflammation (IgE-CAI). IgE-CAI was induced in FcRγ(−/−) mice that received primary basophils from wild-type (WT), FT-IV(−/−), FT-VII(−/−), and FT-IV(−/−)/FT-VII(−/−) mice. (**a**) Although basophils from FT-IV(−/−) and FT-VII(−/−) mice induced exacerbated IgE-CAI as compared with WT basophils, (**b**) FT-IV(−/−)/FT-VII(−/−) mice–derived basophils were incapable of inducing IgE-CAI. *$P<0.05$.

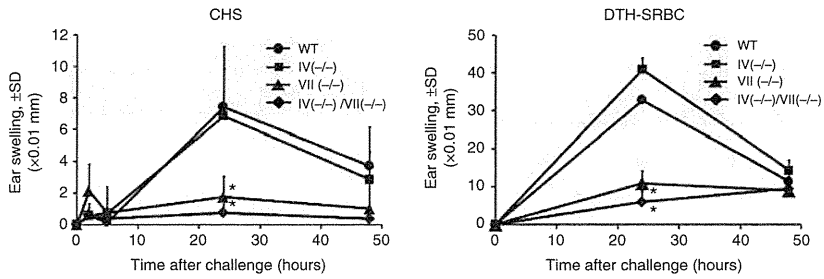

Figure 2. Delayed-type hypersensitivity (DTH) reactions in α(1, 3) fucosyltransferase-IV (FT-IV)- and/or FT-VII-deficient mice. Contact hypersensitivity (CHS) and DTH to sheep red blood cells (DTH-SRBCs) were induced in mice lacking FT-IV and/or -VII. *$P<0.05$ compared with wild-type (WT) mice.

dendritic cells are dispensable for IgE-CAI (Mukai *et al.*, 2005), and thus the development of IgE-CAI in FcRγ(−/−) mice in this experiment could be exclusively mediated by primary basophils. This was also confirmed by the results that IgE-CAI in mice receiving basophil-enriched cell suspension was remarkably alleviated when recipient mice were treated with basophil-depletion antibody (Ba103, kindly provided by Dr Karasuyama (Obata *et al.*, 2007)) (Supplementary Figure S1 online). Basophils from FT-VII(−/−) mice were also capable of inducing IgE-CAI, and interestingly there were higher induction levels as compared with those seen for the WT basophils. This exacerbation was even more marked when basophils were transferred from FT-IV(−/−) mice. Conversely, skin responses in FcRγ(−/−) mice that underwent transfers of primary basophils from FT-IV(−/−)/FT-VII(−/−) mice were completely absent (Figure 3b). Thus, IgE-CAI is entirely dependent on basophil selectin ligands that are collaboratively generated by FT-IV and FT-VII.

Expression of functional selectin ligands on basophils is not sufficient for the full development of IgE-CAI

As inflammatory cells, such as T cells, neutrophils, and eosinophils, have FT-IV and/or FT-VII and are recruited to the skin in a selectin-dependent manner (Homeister *et al.*, 2001; Smithson *et al.*, 2001; Satoh *et al.*, 2005), we examined the development of IgE-CAI by performing experiments designed to assess the contribution of selectin ligands generated by FT-IV/VII in cells other than basophils. WT basophils together with CD49b (−) bone marrow cells (effector cells) from either WT or FT-IV(−/−)/FT-VII(−/−) mice were transferred to irradiated FT-IV(−/−)/FT-VII(−/−) mice. Transfers with the CD49b (−) effector cells from WT mice resulted in a successful induction of IgE-CAI in FT-IV(−/−)/FT-VII(−/−) mice (Figure 4a). Although the CD49b (−) effector cells from FT-IV(−/−)/FT-VII(−/−) mice also induced IgE-CAI responses, induction levels were lower than those of the mice receiving WT mice–derived

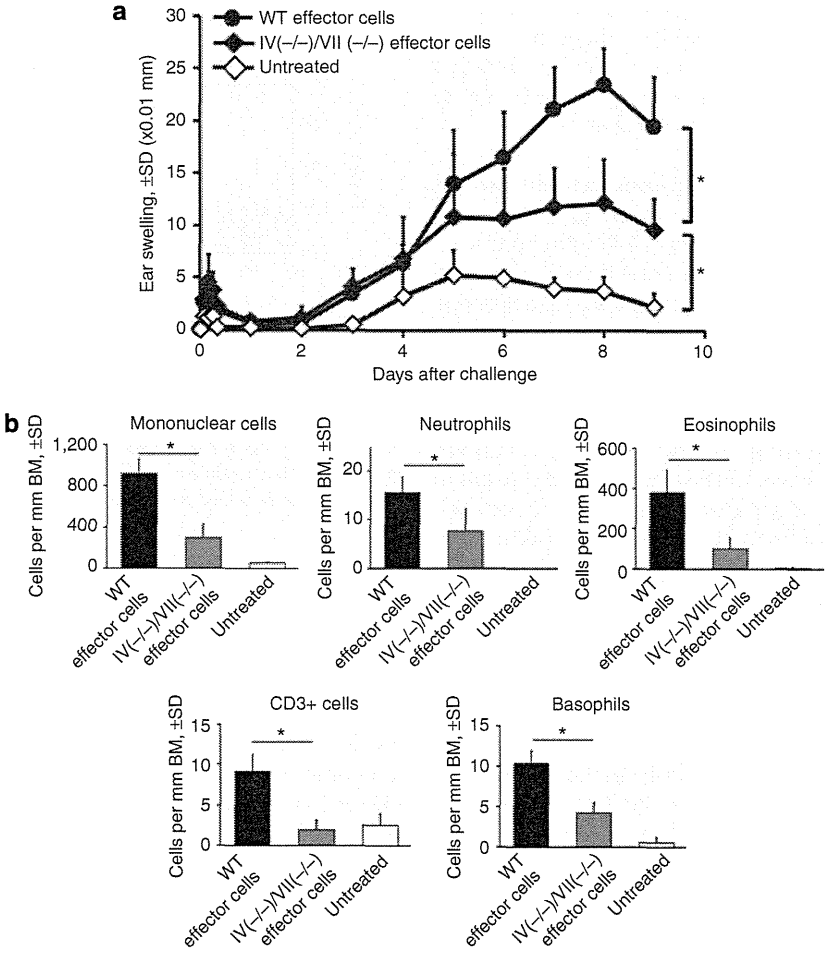

Figure 4. Selectin-dependent cooperative recruitment of basophils and effector cells. (**a**) Irradiated α(1, 3) fucosyltransferase-IV (FT-IV)(−/−)/FT-VII(−/−) mice received wild-type (WT) basophils in combination with CD49b(−) bone marrow cells (effector cells) from either WT or FT-IV(−/−)/FT-VII(−/−) mice. They were then immunized with trinitrophenyl-IgE (TNP-IgE) and challenged with TNP-OVA. The untreated group comprised FT-IV(−/−)/FT-VII(−/−) mice without cell transfer. (**b**) Cell populations in inflammatory skin. *$P<0.05$ compared with WT effector cells. BM, basement membrane.

CD49b (−) effector cells. When cell populations from inflammatory skin were analyzed, it was shown that, even in the presence of WT basophils, there was an impairment of the recruitment of mononuclear cells, neutrophils, CD3 (+) T cells, and eosinophils in mice transferred with FT-IV(−/−)/FT-VII(−/−) mice–derived CD49b(−) effector cells (Figure 4b). More importantly, when WT basophils were cotransferred with CD49b (−) effector cells from FT-IV (−/−)/FT-VII(−/−) mice, complete recruitment into the skin was not achieved. These data suggest that selectin-dependent recruitment of the effector cells appears to be necessary for sufficient responses of IgE-CAI and effective basophil infiltration to occur, even though functional selectin ligand generation in basophils by FT-IV/VII is essential for skin inflammation.

Binding of E- and P-selectins to basophils *in vitro*

Primary basophils expressed transcripts of FT-IV and FT-VII messenger RNA (mRNA; Figure 5a). This was in contrast to bone marrow–derived mast cells, which only expressed extremely low levels of FT mRNA. Although bone marrow–derived basophils had FT transcripts, the levels were much lower than those seen for the primary basophils. Flow cytometry results showed that E- and P-selectin chimeras could bind to primary basophils from WT but not to FT-IV(−/−)/FT-VII(−/−) mice *in vitro* (Figure 5b).

Blockade of E- and/or P-selectins and the amelioration of IgE-CAI

Given the evidence that basophil expression of both E- and P-selectin ligands was dependent upon FT-IV/VII expression, we next attempted to determine the contribution of E- and P-selectins to the actual basophil recruitment. To determine this, we initially examined the effects of blocking Abs against selectins on the development of IgE-CAI. Unexpectedly, we found that blocking of either the E- (clone 10E9.6, BD Bioscience Pharmingen (San Jose, CA), 100 μg per mouse, intravenous) or P- (clone RB40.34, BD Bioscience Pharmingen, 100 μg per mouse, intravenous) selectins did not result in amelioration of IgE-CAI (Supplementary Figure S2 online). Similarly, dual blocking of P- and E-selectins by coadministration of these two Abs also failed to suppress IgE-CAI. These results were in a striking contrast to prior reports demonstrating that the same antibody clones against P- and E-selectins clearly alleviated eotaxin-induced eosinophil accumulation (Satoh *et al.*, 2005) and cutaneous arthus reaction (Yanaba *et al.*, 2003).

Role of P-selectin glycoprotein-1 and L-selectin interaction in basophil recruitment and development of IgE-CAI

Leukocytes express L-selectin, which then interacts with inducible endothelial ligands and contributes to leukocyte rolling (Spertini *et al.*, 1991, 1992; Luscinskas *et al.*, 1994; Tu *et al.*, 1999). Counter-receptor activity of the L-selectin ligand on endothelial cells has been shown to be dependent on the modification by FT-IV and/or VII (Maly *et al.*, 1996; Tu *et al.*, 1999). However, the interaction of basophil L-selectin with ligands modified by endothelial FTs did not seem to be part of the essential pathway for the development of IgE-CAI, as

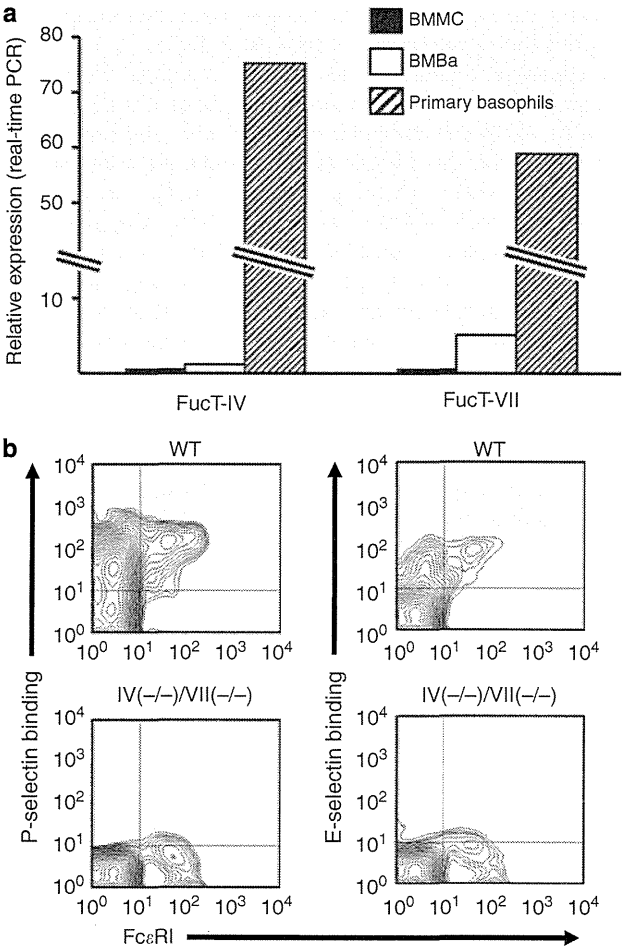

Figure 5. Expression of α(1, 3) fucosyltransferase (FT) messenger RNA (mRNA) and FT-dependent selectin binding in basophils. (**a**) Primary basophils were subjected to further purification by positive selection with CD123 (purity >99%). Transcripts for FT-IV and FT-VII mRNA were quantified by real-time PCR. (**b**) Binding of soluble P- and E-selectins to primary basophils assessed by flow cytometry. BMBa, bone marrow–derived basophil; BMMCs, bone marrow–derived mast cells.

basophils from WT mice were able to successfully induce skin inflammation in FT-IV(−/−)/ FT-VII(−/−) mice lacking counter-receptor activity for L-selectin on endothelial cells (Figure 4a). Prior evidence has also shown that leukocyte PGSL-1, which is a major ligand for P-selectin, can function as a counter-receptor for L-selectin in an FT-dependent manner, thereby contributing to secondary tethering(Guyer *et al.*, 1996; Walcheck *et al.*, 1996). These findings led us to hypothesize that modification of P-selectin glycoprotein-1 (PSGL-1) by FTs in basophils combined with the subsequent binding to L-selectin was an essential pathway for the development of IgE-CAI. To test this hypothesis, we initially confirmed that primary basophils from both WT and FT-IV(−/−)/FT-VII(−/−) mice expressed PSGL-1 and L-selectin on their cell surface (Figure 6a). PSGL-1 Ab (4RA10, BD Bioscience Pharmingen) almost completely inhibited the *in vitro* binding